

1D and 2D Cobalt(II) Coordination Polymers, Co(ox)(en): Synthesis, Structures and Magnetic Properties

Jaeyun Kang, Yumi Lee, Seungjoo Kim,[†] Hoseop Yun,[†] and Junghwan Do^{*}

Department of Chemistry, Konkuk University, Seoul 143-701, Korea. *E-mail: junghwan@konkuk.ac.kr

[†]Department of Chemistry, Ajou University, Suwon 441-749, Korea

Received June 16, 2014, Accepted July 18, 2014

Two ethylenediamine cobalt(II) oxalate complexes Co(ox)(en), **1** and Co(ox)(en)·2H₂O, **2** have been hydrothermally synthesized and characterized by single crystal X-ray diffraction, IR spectrum, TG analysis, and magnetic measurements. In **1**, Co atoms are coordinated by two bis-bidentate oxalate ions in *trans*-configuration to form Co(ox) chains, which are further bridged by ethylenediamine molecules to produce 2D grid layers, Co(ox)(en). In **2**, Co atoms are coordinated by bridging oxalate ions in *cis*-configuration to form Co(ox) chains, and the additional chelation of ethylenediamine to Co atoms completes 1D zigzag chain, Co(en)(ox). Two lattice water molecules stabilize the chains through hydrogen bonding. Magnetic susceptibility measurements indicate that both complexes exhibit weak antiferromagnetic coupling between cobalt(II) ions with the susceptibility maxima at 23 K for **1** and 20 K for **2**, respectively. In **1** and **2**, the oxalate ligands afford a much shorter and more effective pathway for the magnetic interaction between cobalt ions compared to the ethylenediamine ligands, so the magnetic behaviors of both complexes could be well described with 1D infinite magnetic chain model.

Key Words : Hydrothermal synthesis, Cobalt complex, Oxalate, Ethylenediamine, Magnetic properties

Introduction

Metal oxalate complexes exhibit molecular based magnetism where the oxalate mediates magnetic exchanges by bridging paramagnetic first-row transition metal cores. The oxalate units mainly adopt two types of bridging modes of *cis*- and *trans*-configuration on an octahedrally coordinated metal center. Depending on orbital topology followed by the magnetic cores, counter cations, and the bridging ligands, these compounds show ferromagnetic or antiferromagnetic couplings with various exchange coupling *J* values. Several 1D and 2D metal oxalate complexes with mixed bridging ligands were synthesized and magnetically characterized. In general, the 1D polymers possess zigzag or linear types depending on the configuration of oxalate ligands on metal centres. The octahedral coordinate in zigzag chains can adopt terminal ligand positions by monodentate or chelating bidentate ligands, while linear chains can only adopt monodentate ligands.¹⁻¹⁷ On the other hand, 2D layered structures contain bridging multidentate ligands such as 2,2'-bipyrimidine, pyrazine, and 4,4'-bipyridine (bpy), which are obviously different from chelating bidentate ligands found in 1D structures.¹⁸⁻²⁵ The geometric patterns of the layers are essentially distinguished by the facility and number of chelating ligands in the structures. For instance, the constitution ratio of metal oxalate to bidentate ligand in M(ox)(bpy) (M=Fe, Co, Ni, Zn),²¹ Cu₂(ox)₂(pyz)₃,²⁰ and M₃(ox)₃(bpy)₄ (M=Fe, Mn, Cu, Zn)²²⁻²⁵ are 1:1, 2:3, and 3:4, respectively. The first contains linear chains of metal oxalate, all which are cross-linked by bpy in a perpendicular manner, leading to square grid layers with rectangular windows, whereas the

second and third include puckered chains of metal oxalate linked by both terminal and bridging ligands.

Here we report the synthesis, structures, and magnetic properties of two ethylenediamine cobalt(II) oxalate complexes, Co(ox)(en) **1** and Co(ox)(en)·2H₂O **2**. In **1** the cobalt atoms are bridged by ethylenediamine and oxalate ligands, both in *trans*-configuration to produce 2D grid layer Co(ox)(en) with rhomboidal windows. In **2** each cobalt atom is capped by one ethylenediamine molecule and is bridged by two oxalate ligands in a *cis*-configuration to complete the zigzag chain structure. Compound **2** is isostructural to M(ox)(en)·2H₂O (M=Zn, Ni).^{26,27}

Experimental

Materials and Measurements. All chemicals used during this work were of reagent grade and used as received from commercial sources without further purification. Thermal analyses were carried out in N₂ at a heating rate of 5 °C/min, using a high-resolution Perkin-Elmer TGA7 Thermal Analyzer and Perkin-Elmer Diamond DSC. Infrared spectra were recorded on a Nicolet 6700 FT-IR spectrometer within a range of 400–4000 cm⁻¹ using the KBr pellet method. Qualitative analyses of the compounds were performed with JEOL JSM-5200 SEM equipped with an EDAX Genesis EDS detector. Element analyses of the compounds were carried out using ThermoQuest CE EA 1110 for C, H, and N. Magnetic susceptibilities were measured in the temperature range 5 K ≤ T ≤ 300 K at applied field of 10 kG using a Quantum Design MPMS XL SQUID magnetometer installed at Korean Basic Science Institute. The samples were

Table 1. Crystal data and structure refinement for **1** and **2**

	1	2
Formula	C ₄ H ₈ CoN ₂ O ₄	C ₄ H ₁₂ CoN ₂ O ₆
Formula weight	207.05	243.09
T, K	293(2)	293(2)
Crystal size (mm)	0.32 × 0.27 × 0.22	0.27 × 0.21 × 0.16
Space group	C2/m	C2/c
<i>a</i> , Å	7.657(1)	12.012(2)
<i>b</i> , Å	8.355(2)	8.987(2)
<i>c</i> , Å	5.497(1)	9.332(2)
β , deg	108.28(3)	115.30(3)
<i>V</i> , Å ³	333.9(1)	910.8(3)
<i>Z</i>	2	4
<i>D</i> _{calcd} , g/cm ³	2.060	1.773
μ , mm ⁻¹	2.534	1.887
<i>F</i> (000)	210	500
GOF on <i>F</i> ²	1.235	1.130
R index (<i>I</i> > 2 σ (<i>I</i>))	R1 = 0.0266, wR2 = 0.0719	R1 = 0.0277, wR2 = 0.0709
R index (all data)	R1 = 0.0271, wR2 = 0.0720	R1 = 0.0327, wR2 = 0.0759
($\Delta\rho$) _{max:min} , e/Å ³	0.814: -0.373	0.658: -0.467

contained in a gelatin capsule fastened in a plastic straw for immersion into the SQUID. The susceptibility data were corrected for the magnetization of the sample holder.

Synthesis of Co(ox)(en), 1. Compound **1** was synthesized from a mixture of Co₃O₄ (0.0582 g, 0.24 mmol), oxalic acid (0.018 g, 0.2 mmol), ethylenediamine (0.039 mL, 0.6 mmol), and water (0.6 mL) which was sealed under vacuum in a Pyrex tube and heated to 150 °C for 2 days, followed by cooling to 30 °C at 10 °C/h. The solution pH values before and after the reaction were ~7 and ~8, respectively. The solid products were recovered by vacuum filtration and washed with water. Brown polyhedral crystals of Co(ox)(en) and unidentified white powder were found. The yield of the product, Co(ox)(en), **1** was 62% based on cobalt. The products were stable in air and insoluble in water, common polar and non-polar solvents. EDS analysis confirmed the presence of Co. The element analyses gave the following results: obsd. (wt %) (C, 23.09; H, 4.02; N, 13.67), calcd (wt %) (C, 23.20; H, 3.89; N, 13.53). IR (KBr): 3311m, 3262w, 2979w, 2914w, 1627s, 1478w, 1361m, 1316m, 1100m, 1017s, 796m, 600w, 490m, 442w cm⁻¹.

Synthesis of Co(ox)(en)·2H₂O, 2. Compound **2** was prepared from a solution of Co(CH₃COO)·4H₂O (0.249 g, 1.0 mmol), ethylenediamine (0.14 mL, 2.0 mmol) in distilled water (3 mL), which was placed in a 10 mL screw-capped tube. Oxalic acid (0.090 g, 1.0 mmol) was dissolved in ethanol (3 mL) and layered on top. Red polyhedral crystals of Co(ox)(en)·2H₂O and unknown yellowish orange micro-crystals were observed at the interface after ~10 d of inter-diffusion. The products were stable in air and insoluble in water, common polar and non-polar solvents. EDS analysis confirmed the presence of Co. The element analyses gave the following results: obsd. (wt %) (C, 19.91; H, 5.01; N,

11.45), calcd (wt %) (C, 19.76; H, 4.98; N, 11.52). IR (KBr): 3504m, 3427m, 3325w, 3281w, 1698m, 1614s, 1352w, 1316m, 1100w, 1034m, 801m, 619w, 506m cm⁻¹.

X-ray Structure Determination. Single-crystal data were collected on a Rigaku R-Axis RAPID diffractometer (graphite-monochromated MoK α radiation, λ = 0.71073 Å, T = 150 K): The structure was solved by direct methods using SHELXS97, refined on *F*² by full-matrix least squares using SHELXL97.²⁸ The data for **1** and **2** were corrected for absorption using the multi-scan method.²⁹ Hydrogen atoms associated with the ethylenediamine molecules in **1** and **2** were placed geometrically and refined by riding. The H atoms of the water molecule in **2** were located in a Fourier difference map and were refined freely. All non-hydrogen atoms were refined anisotropically. Further details of the X-ray structural analysis are given in Table 1.

Results and Discussion

Structure of Co(ox)(en), 1. The structure of **1** is built up of infinite neutral Co(ox)(en) (ox = oxalate; en = ethylenediamine) layers. One unique cobalt atom is coordinated by four oxygen atoms in two oxalate ions and two nitrogen atoms in two ethylenediamine molecules to form a slightly distorted octahedral geometry in the range of 2.118(2)–2.166(2) Å. The BVS calculation gives a value of 2.09 for Co, indicating an oxidation state of +2.00.³⁰ The oxalate ions acting as bis-bidentate ligands link cobalt atoms in *trans*-configuration forming a Co(ox) chain along the *c* direction. The cobalt atoms in the chain are further bridged by ethylenediamine molecules in *trans*-configuration to complete 2D Co(ox)(en) layer (Figure 1). The Co(ox)(en) layer contains large rhomboid-shaped voids with cross section *a* (7.657(2) Å) × *c* (5.497(1) Å), enclosed by four Co atoms located at the corners of the rhomboid. The ethylenediamine shows an *anti*-conformation (crystallographic two-fold symmetry, N–C–N torsional angle = 180.0°), a phenomenon

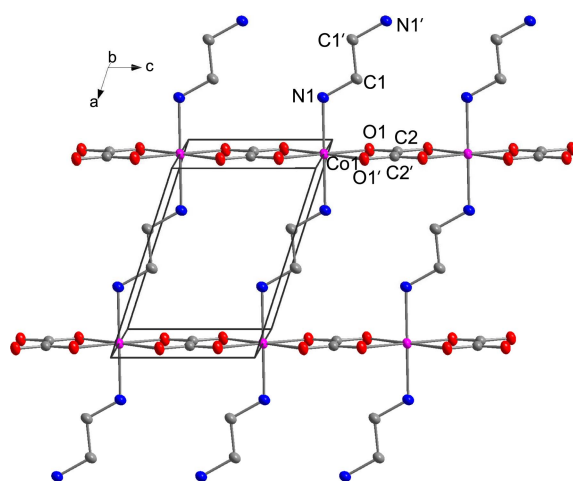


Figure 1. Displacement ellipsoids of the Co(ox)(en) layer in **1**, drawn at 50% probability level. The pink, grey, blue, and red atoms are Co, C, N, and O, respectively. Hydrogen atoms are omitted for clarity.

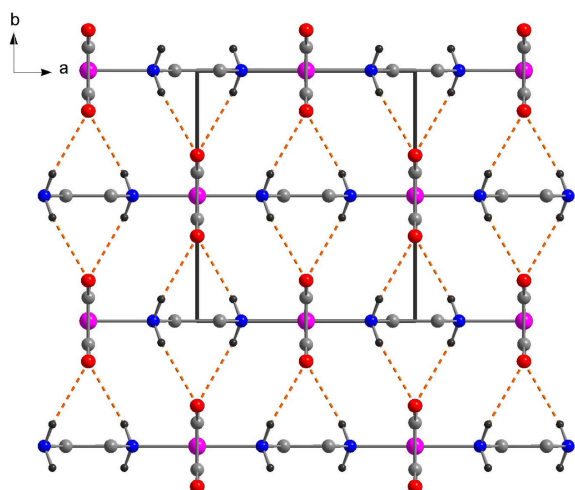


Figure 2. Frameworks formed in **1** by hydrogen bonding (dotted red lines) between the layers. Hydrogen atoms in N atoms are represented by black spheres. Hydrogen atoms in C atoms are omitted for clarity.

that is commonly found in bridging ethylenediamine ligands. The adjacent layers are shifted by $\frac{1}{2}a \sim 3.83 \text{ \AA}$, and the distance between the two adjacent layers is $\frac{1}{2}b \sim 4.18 \text{ \AA}$. Weak hydrogen bonds are found between the layers, $d(\text{N1} \cdots \text{O1}) = 3.2230(6) \text{ \AA}$ (Figure 2).

It is notable to compare with $\text{M}(\text{ox})(\text{bpy})$ ($\text{M} = \text{Fe}, \text{Co}, \text{Ni}, \text{Zn}$), which show similar layered structures.²¹ These contain linear $\text{M}(\text{ox})$ chains that are cross-linked by 4,4'-bipyridine in a perpendicular manner, leading to square grid layers with rectangular windows. The approximate dimensions of the rectangular voids in the $\text{Co}(\text{ox})(\text{bpy})$ layer are $11.4 \times 5.4 \text{ \AA}^2$. The interlayer distance of 5.50 \AA in $\text{Co}(\text{ox})(\text{bpy})$ is much longer than 4.18 \AA in **1**. The adjacent square grid layers of $\text{Co}(\text{ox})(\text{bpy})$ are shifted diagonally by $\frac{1}{2}a + \frac{1}{2}c$, whereas the adjacent layers are shifted axially by $\frac{1}{2}a$ in **1**. The dissimilar interlayer distance and shift in interlayer packing arrangement arise from the steric requirement of the bridging diamine ligands between the $\text{Co}(\text{ox})$ chains, *i.e.*, short and small ethylenediamine and longer and more bulky 4,4'-bipyridine.

Structure of $\text{Co}(\text{ox})(\text{en}) \cdot 2\text{H}_2\text{O}$, **2.** The crystal structure of **2** is built up of infinite neutral $\text{Co}(\text{ox})(\text{en})$ chains separated by lattice water molecules. One crystallographically independent cobalt atom is coordinated by four oxygen atoms in two oxalate ions and two nitrogen atoms in one ethylenediamine molecule to form a slightly distorted octahedral geometry in the range of $2.108(2)$ – $2.129(2) \text{ \AA}$. The BVS calculation gives a value of 2.19 for Co, indicating an oxidation state of +2.00. Unlike **1**, oxalate ions acting as bis-bidentate ligands connect cobalt atoms in a *cis*-configuration producing zigzag $\text{Co}(\text{ox})$ chains along the *c* direction, which enforce the additional ethylenediamine molecule to chelate the Co atoms forming zigzag $\text{Co}(\text{ox})(\text{en})$ chains (Figure 3). The interchain space is filled by water molecules that link the chains through hydrogen bonds of $d(\text{Ow} \cdots \text{O2}) = 2.765 \text{ \AA}$ and $d(\text{Ow} \cdots \text{O1}) = 2.884 \text{ \AA}$, which results in the formation of a 3D network structure (Figure 4). No hydro-

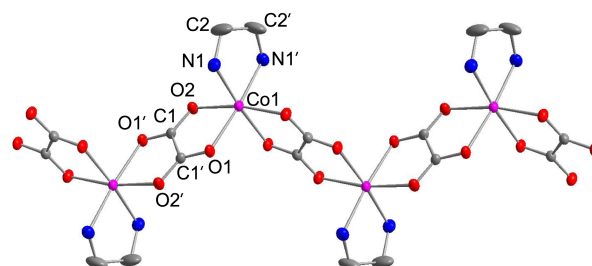


Figure 3. Displacement ellipsoids of the $\text{Co}(\text{ox})(\text{en})$ chain in **2**, drawn at 50% probability level. The labeling scheme is the same as that in figure 1. Hydrogen atoms of ethylenediamine molecules are omitted for clarity.

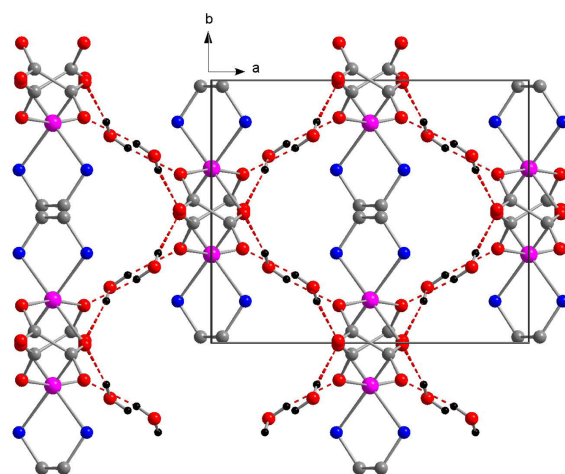


Figure 4. View of **2** showing the framework formed through hydrogen bonding. The labeling scheme is the same as that in figure 2. Hydrogen atoms of ethylenediamine molecules are omitted for clarity.

gen bonds are found between the lattice water molecules and nitrogen atoms in ethylenediamine within 3.1 \AA . Also, no hydrogen bonds between water molecules are observed within 4.0 \AA .

Characterization. The IR spectrum for **1** exhibits the characteristic features of the oxalate anion: $\nu_{\text{as}}(\text{CO}_2)$ at 1627s cm^{-1} , $\nu_{\text{s}}(\text{CO}_2)$ at 1361m and 1316m cm^{-1} , $\nu_{\text{s}}(\text{CO})$ at 1100m and 1017s cm^{-1} , $\delta(\text{CO}_2)$ at 796m cm^{-1} . Vibration modes for Co–O and Co–N are observed at 600w , 490m , and 442w cm^{-1} . Additional bands at 3311m , 3262w , 2979w , 2914w and 1478w cm^{-1} are due to the N–H, C–H, C–C, and C–N vibrations. The IR spectrum for **2** shows similar features as **1**: $\nu_{\text{as}}(\text{CO}_2)$ at 1698m and 1614s cm^{-1} , $\nu_{\text{s}}(\text{CO}_2)$ at 1352w and 1316m cm^{-1} , $\nu_{\text{s}}(\text{CO})$ at 1100w and 1034m cm^{-1} , $\delta(\text{CO}_2)$ at 801m cm^{-1} . Vibration modes for Co–O and Co–N are observed at 619w and 506m cm^{-1} . Additional bands at 3504m , 3427m , 3325w and 3281w cm^{-1} are due to the N–H, O–H, C–H, C–C, and C–N vibrations.

Simulated powder X-ray patterns based on the single-crystal structures were in excellent agreement with the X-ray powder data. The thermal stability of **1** was probed using thermogravimetric analysis. The TG analysis showed that upon heating in N_2 , **1** remained stable up to $\sim 300 \text{ }^\circ\text{C}$. On

further heating, a sharp weight loss of 61.10% occurred in the range of 300–500 °C, which was attributed to the evolution of ethylenediamine, CO, and CO₂ molecules. Assuming that the residue at 800 °C corresponds to Co₃O₄, the overall observed weight loss of 61.10% is in good agreement with that calculated value of Co₃O₄ (61.23%). The final product of Co₃O₄ was confirmed by Powder-XRD.

The thermal decomposition of **2** occurs in two steps from room temperature to 800 °C. The first step below 100 °C corresponds to the loss of the two lattice water molecules (weight loss: calcd., 14.81%; obs., 15.38%). The dehydrated material, Co(en)(ox) is stable up to ~350 °C. Above this the evolution of ethylenediamine, CO, and CO₂ molecules occurs. Assuming that the residue at 800 °C corresponds to Co₃O₄, the overall observed weight loss of 67.20% is in good agreement with the calculated value of Co₃O₄ (66.98%). The final product of Co₃O₄ was confirmed by Powder-XRD.

In general, the chelating ethylenediamine possess greater binding energy than that of bridging, as usually indicated by the shorter M–N distance, which results in higher decomposition temperature of the chelating ethylenediamine than those of bridging ethylenediamine. Examples include *rac*-μ-en[*cis*-CoCl(en)₂]₂(ZnCl₄)₂, [Pb(en)₂]Br₂ and Pb(en)₂Cl₂.^{31–33} For instance, in Pb(en)₂Cl₂, the bond length of Pb to N atom in the chelating ligand (2.447(3) Å) is significantly shorter than that of the bridging ligand (2.602(3) Å).³³ Therefore, the range of decomposition temperatures for chelating and bridging ethylenediamine molecules are clearly distinguished: the chelating ethylenediamine (150–320 °C) decomposes at a higher temperature than bridging ethylenediamine (80–150 °C). Compounds **1** and **2** however, show similar bond lengths (for **1**, bridging ~320–450 °C, d(Co–N) = 2.166(2) Å; for **2**, chelating ~330–450 °C, d(Co–N) = 2.129(2) Å), and indicate similar decomposition temperatures of ethylenediamine molecules in the structures.

Magnetic Properties. The temperature dependences of the magnetic susceptibility for **1** and **2** are represented in Figure 5. The magnetic susceptibilities (χ_m) increase when the compounds are cooled until maxima are reached at 23 K for **1** and 20 K for **2**, respectively, and then decrease. In the $\chi_m T$ vs. T plots, downward curvatures are observed with decreasing temperature. These are characteristics of antiferromagnetic interactions. Similar aspects were reported for cobalt (II) complexes showing a moderate antiferromagnetic coupling between the metal centers through the bridging oxalate ligand.^{34–36} Fitting the high temperature susceptibility (50 K ≤ T ≤ 300 K) to the Curie–Weiss law results in values of $\mu_{\text{eff}} = 5.22 \mu_B$ for **1** and $\mu_{\text{eff}} = 5.24 \mu_B$ for **2**. The magnetic properties of high spin octahedral cobalt (II) complexes are governed by the orbitally degenerate ground term, ⁴T_{1g}. This provides an orbital contribution to the magnetic moment which is much larger than that expected for the spin-only value of 3.87 μ_B . The effective magnetic moments for **1** and **2** are comparable to those in the range of 4.7–5.9 μ_B observed for compounds containing uncoupled high spin octahedral cobalt (II) ion.³⁷

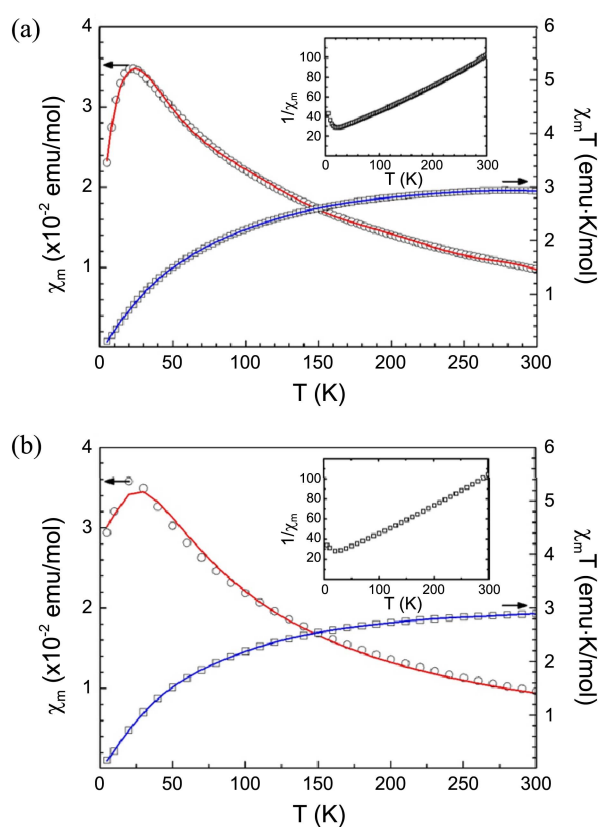


Figure 5. χ_m vs. T and $\chi_m T$ vs. T plots measured in an applied field of 10 kG for the Co(ox)(en) **1** (a), Co(ox)(en)·2H₂O **2** (b). The measured values are represented by empty circles (χ_m) and empty squares ($\chi_m T$). Their best theoretical fits are represented by solid lines. Insets are $1/\chi_m$ vs. T plots for **1** and **2**, respectively.

In **1**, Co atoms are coordinated by two oxalate ions in *trans*-configuration, which are further bridged by ethylenediamine molecules to produce 2D grid layers. The ethylenediamine ligands cause Co–Co distances to become too long for any significant magnetic interaction. On the other hand, a much more favorable Co–oxalate–Co superexchange path is apparent. Namely, the Co–Co distance along in the *c* direction is considerably smaller (*c.a.* 5.497 Å) than the Co–Co distance (*c.a.* 7.657 Å) along the *a* direction. The structure of **1**, therefore, can be considered as the magnetic chains running along the *c* axis, although it belongs to the crystallographically 2D system. In **2**, each Co atom is coordinated by bridging oxalate ions in *cis*-configuration to form a 1D zigzag chain. The nearest Co–Co distance in **2** is 5.512 Å which is nearly identical with the Co–Co distance in **1**.

The experimental susceptibility data for **1** and **2** were fitted to an infinite chain model derived by Fisher:^{38,39}

$$\chi_m = \frac{Ng^2 \beta S(S+1)}{3kT} \frac{1+u}{1-u}$$

with

$$u = \coth \left[\frac{JS(S+1)}{kT} \right] - \left[\frac{kT}{JS(S+1)} \right]$$

The best fits gave $g = 2.5$, $J = -11.8 \text{ cm}^{-1}$ for **1** and $g = 2.6$,

$J = -10.3 \text{ cm}^{-1}$ for **2**. The J parameters are in agreement with other values previously found in different Co chain systems through the same magnetic model; $J = -9.3 \text{ cm}^{-1}$ for $[\text{Co}(\text{ox})\text{L}_2 \cdot 2\text{H}_2\text{O}]$ ($\text{L} = 1,2,4\text{-triazole}$),³⁴ $J = -20.9 \text{ cm}^{-1}$ for $[\text{Co}(\text{ox})(\text{H}_2\text{O})_2]^{35}$ and $J = -14.2 \text{ cm}^{-1}$ for $[\text{Co}(\text{ox})(\text{H}_2\text{O})_2] \cdot 2\text{H}_2\text{O}$.³⁶ The slightly larger magnitude of the parameter $|J|$ of **1** compared to **2** indicates that the magnetic exchange between cobalt ions may be mediated more effectively by the *trans*-configuration than by the *cis*-configuration of oxalate ligands.

Conclusion

In conclusion, we have synthesized and characterized two ethylenediamine cobalt(II) oxalate complexes, 2D-Co(ox)(en) **1** and 1D-Co(ox)(en)·2H₂O **2**. The structural difference arises from the different configuration of oxalate ions in octahedral site, *i.e.*, *trans*- and *cis*-, and due to the chelating or bridging roles of the ethylenediamine ligands. The *trans*-configuration of linear Co(ox) chains allows the ethylenediamine molecules cross-bridging the chains in almost perpendicular manner to complete 2D Co(ox)(en) grid layers, while *cis*-configuration of zigzag Co(ox) chains embraces chelating ethylenediamine to produce 1D Co(ox)(en) chains. Both Co(II) coordination polymers **1** and **2** are found to show weak antiferromagnetic interactions between cobalt ions, which can be described with 1D magnetic chain model. The comparison of the T_N and J parameters for two complexes suggests that the magnetic interaction of cobalt ions *via trans*-oxalate ligands is slightly stronger than that *via cis*-oxalate ligands.

Acknowledgments. This paper was supported by Konkuk University in 2011.

Supplementary Materials. Crystallographic data for the structures reported here have been deposited with CCDC (Deposition No. CCDC-1001492 (**1**) and CCDC-1001493 (**2**)). These data can be obtained free of charge *via* <http://www.ccdc.cam.ac.uk/conts/retrieving.html> or from CCDC, 12 Union Road, Cambridge CB2 1EZ, UK, E-mail: deposit@ccdc.cam.ac.uk

References

1. Yu, J.-H.; Xu, J.-Q.; Zhang, L.-J.; Lu, J.; Zhang, X.; Bie, H.-Y. *J. Mol. Struct.* **2005**, *743*, 243.
2. Jiang, Y.-C.; Wang, S.-L.; Lee, S.-F.; Lii, K.-H. *Inorg. Chem.* **2003**, *42*, 6154.
3. Fang, F.-Y.; Guo, X.-X.; Song, W.-D. *Acta Crystallogr.* **2007**, *E63*, m1031.
4. Coronado, E.; Giménez, M. C.; Gómez-García, C. J.; Romero, F. M. *Polyhedron* **2003**, *22*, 3115.
5. Román, P.; Guzmán-Miralles, C.; Luque, A.; Beitia, J. I.; Cano, J.; Lloret, F.; Julve, M.; Alvarez, S. *Inorg. Chem.* **1996**, *35*, 3741.
6. Wang, L.-M.; Chu, D.-Q.; Pan, C.-L. *Mendeleev Commun.* **2002**, *12*, 235.
7. Yu, J.-H.; Hou, Q.; Bi, M.-H.; Lü, Z.-L.; Zhang, X.; Qu, X.-J.; Lu, J.; Xu, J.-Q. *J. Mol. Struct.* **2006**, *800*, 69.
8. García-Terán, J. P.; Castillo, O.; Luque, A.; García-Couceiro, U.; Román, P.; Lloret, F. *Inorg. Chem.* **2004**, *43*, 5761.
9. Ghost, S. K.; Savitha, G.; Bharadwaj, P. K. *Inorg. Chem.* **2004**, *43*, 5495.
10. Castillo, O.; Luque, A.; Román, P.; Lloret, F.; Julve, M. *Inorg. Chem.* **2001**, *40*, 5526.
11. Oshio, H.; Nagashima, U. *Inorg. Chem.* **1992**, *31*, 3295.
12. Xia, S. Q.; Hu, S. M.; Dai, J. C.; Wu, X. T.; Fu, Z. Y.; Zhang, J. J.; Du, W. X. *Polyhedron* **2004**, *23*, 1003.
13. Hernández-Molina, M.; Lorenzo-Luis, P. A.; Ruiz-Pérez, C. *CrystEngComm* **2001**, *16*, 1.
14. Lu, J. Y.; Schroeder, T. J.; Babb, A. M.; Olmstead, M. *Polyhedron* **2001**, *20*, 2445.
15. Lu, J. Y.; Babb, A. *Inorg. Chim. Acta* **2001**, *318*, 186.
16. Ferjani, J.; Graia, M.; Jouini, T. *Acta Crystallogr.* **2005**, *C61*, m237.
17. Hong, C. S.; Yoon, J. H.; You, Y. S. *Inorg. Chem. Commun.* **2005**, *8*, 310.
18. Armentano, D.; De Munno, G.; Lloret, F.; Julve, M.; Curely, J.; Babb, A. M.; Lu, J. Y. *New J. Chem.* **2003**, *27*, 161.
19. De Munno, G.; Ruiz, R.; Lloret, F.; Faus, J.; Sessoli, R.; Julve, M. *Inorg. Chem.* **1995**, *34*, 408.
20. Kitagawa, S.; Okubo, T.; Kawata, S.; Kondo, M.; Katada, M.; Kobayashi, H. *Inorg. Chem.* **1995**, *34*, 4790.
21. Lu, J. Y.; Lawandy, M. A.; Li, J.; Yuen, T.; Lin, C. L. *Inorg. Chem.* **1999**, *38*, 2695.
22. Castillo, O.; Alonso, J.; Garcia-Couceiro, U.; Luque, A.; Roman, P. *Inorg. Chem. Commun.* **2003**, *6*, 803.
23. Zheng, L.-M.; Fang, X.; Lii, K.-H.; Song, H.-H.; Xin, X.-Q.; Fun, H.-K.; Chinnakali, K.; Razak, I. A. *J. Chem. Soc., Dalton Trans.* **1999**, 2311.
24. Zhu, L.-H.; Zeng, M.-H.; Ng, S. W. *Acta Crystallogr.* **2005**, *E61*, m916.
25. Nordell, K. J.; Higgins, K. A.; Smith, M. D. *Acta Crystallogr.* **2003**, *E59*, m114.
26. Van Albada, G. A.; Mohamadou, A.; Mutikainen, I.; Turpeinen, U.; Reedijk, J. *Acta Crystallogr.* **2004**, *E60*, m1160.
27. Chun, J.; Lee, Y.; Pyo, S.; Im, C.; Kim, S.-J.; Yun, H.; Do, J. *Bull. Korean Chem. Soc.* **2009**, *30*, 1603.
28. Sheldrick, G. M. *Acta Crystallogr.* **2008**, *A64*, 112.
29. Rigaku *RAPID-AUTO Manual*, Rigaku Corporation: Tokyo, Japan 2006.
30. Brese, N. E.; O'Keeffe, M. *Acta Crystallogr.* **1991**, *B47*, 192.
31. Harrowfield, J. M.; Miyamae, H.; Shand, T. M.; Skelton, B. W.; Soudi, A. A.; White, A. H. *Aust. J. Chem.* **1996**, *49*, 1043.
32. House, D. A.; Steel, P. J. *Inorg. Chim. Acta* **1999**, *288*, 53.
33. Cho, Y.; Kim, S.; Pyo, S.; Park, Y.-S.; Kim, S.-J.; Yun, H.; Do, J. *Polyhedron* **2010**, *29*, 2105.
34. Olea, D.; Garcia-Couceiro, U.; Castillo, O.; Gomez-Herrero, J.; Zamora, F. *Inorg. Chim. Acta* **2007**, *360*, 48.
35. Lukin, J. A.; Simizu, S.; Vandervan, N. S.; Friedberg, S. A. *J. Magn. Magn. Mater.* **1995**, *140*, 1669.
36. Garcia-Couceiro, U.; Castillo, O.; Luque, A.; Beobide, G.; Roman, P. *Inorg. Chim. Acta* **2004**, *357*, 339.
37. Mabbs, F. E.; Machin, D. J. *Magnetism and Transition Metal Complexes*; Chapman and Hall: 1973.
38. Fisher, M. E. *Am. J. Phys.* **1964**, *32*, 343.
39. Khan, O. *Molecular Magnetism*; VCH publisher: 1993.